Macromolecules

ARTICLE

pubs.acs.org/Macromolecules

Donor−Acceptor Intermediates and Low-Bandgap Polymers by Electropolymerization of Thienoazaborines

Olena Lukoyanova,* Marc Lepeltier, Marie Laferrière, and Dmitrii F. Perepichka*

Department of Chemistry, McGill University, Montreal, Quebec, H3A 2K6

Supporting Information

ABSTRACT: New low-bandgap polythiophenes ($E_g \sim 1.2$ eV) with thienoquinodiimine and diphenylbithiophene alternating moieties were synthesized via electrochemical polymerization of azaborines **1a** and **1b**. The polymers were investigated by cyclic voltammetry (CV), differential pulse voltammetry (DPV), vis−NIR spectroelectrochemistry, and X-ray photoelectron spectroscopy (XPS). Formation of these polymers is accompanied by boron expulsion from the fused dithienoazaborine system and formation of a new C−C bonds between thiophene backbone and phenyl substituents. This finding was supported by isolating the intermediates **2** and **3** with partially deborylated structures. The optoelectronic properties of the later, investigated by UV−vis spectroscopy and CV, are controlled by the interaction between the donor (amino-substituted thiophene) and acceptor (thienoazaborine) moieties which is weak in the ground state due to twisted structure of the molecule but is enhanced in the excited state leading to large fluorescence Stokes shift.

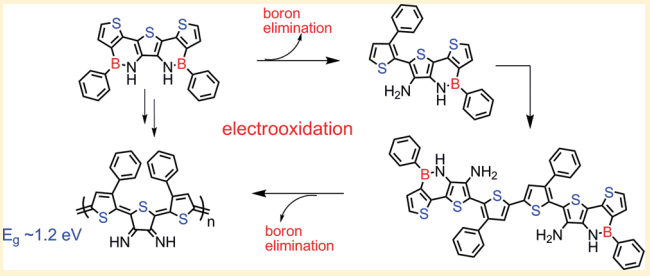

INTRODUCTION

Electrochemical oxidative polymerization has long been used to synthesize conjugated polymers from a variety of electron-rich (hetero)aromatic monomers—anilines, pyrroles, thiophenes, and a few others.[1] It is particularly attractive and almost unique for insoluble conjugated polymers (those lacking solubilizing groups) as it delivers a film of a polymer directly on an electrode, ready for the targeted application. Over the past decade there has been a significant interest in preparing highly functionalized conjugated polymers by electropolymerization of corresponding monomers and oligomers that led to a large structural and functional diversity of the resulting films.[2−11] However, as the complexity of the corresponding monomer increases, the exact structure of the polymer, usually assumed to be a simple repetition of the monomer building block, might be difficult to establish with certainty. Furthermore, the insoluble nature of such polymers hampers standard characterization approaches.

Recently, incorporation of boron into electron-rich conjugated materials has attracted a lot of attention, due to its ability to reduce the LUMO energy and enhance the emissive properties of the materials.[12] Many novel and desirable properties have been demonstrated for such materials, e.g., enhanced electron transport, efficient photo- and electroluminescence, nonlinear optical effect, fluoride/cyanide sensing, etc.[13−17] While strong Lewis acidity of boron is a certain concern for the stability of organoboron materials, a significant progress has been made to reduce its reactivity by substitution of the boron center with bulky substituents, boron inclusion into polycyclic structures,[18] or incorporation of the B−N linkage into a heterocyclic ring system.[19,20] However, only a few reports exploit the ability of electron-rich organoboron monomers to electropolymerize, including some interesting structures such as polythiophenes with boronic acid as a pendant group[21,22] or boron-containing BODIPY derivative as a part of conjugated backbone.[10]

Fused thienoazaborines were first synthesized by Gronowitz et al.[23] We have also recently reported planar fused thienoazaborine systems **1a**,**b** where the boron orbital is stabilized through interaction with the lone pair of the neighboring nitrogen.[24] Here we describe an unusual electrochemical polymerization of the thienoazaborines **1** leading to expulsion of boron and formation a low-band gap polymer **4**. We show how comprehensive spectroscopic characterization and isolation of intermediates (partially deborylated donor−acceptor oligomers **2** and **3**) help in elucidating the structure of an insoluble polymer with unexpected structure.

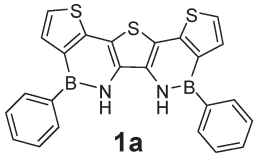

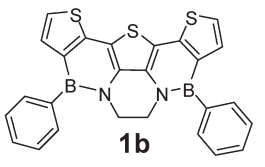

EXPERIMENTAL SECTION

Instrumentation. NMR was performed on Varian Mercury 300 and 500 MHz spectrometers. The UV−vis measurements were done using Varian Cary 5000 spectrometer, and fluorescence spectra were measured with a Varian Eclipse spectrofluorometer. FTIR were obtained using Nicolet 6700 FTIR spectrometer from Thermo Scientific in a

Received: March 4, 2011
Revised: April 27, 2011
Published: May 26, 2011

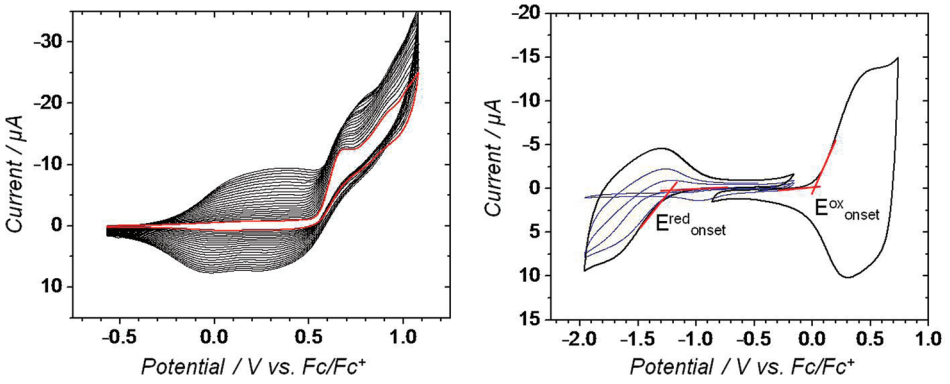

Figure 1. (a) CVs of potentiodynamic growth of polymer film on Pt disk electrode from the solution of **1a** in toluene/acetonitrile, 0.1 M Bu_4NPF_6, 40 mV/s. (b) CV of films electropolymerized from **1a** on Pt disk electrode in CH_2Cl_2/ Bu_4NPF_6; 100 mV/s.

single bounce ATR mode. High resolution mass spectra were obtained using Orbitrap spectrometer from ThermoFisher. All electrochemical experiments were performed at room temperature using a CHI-770 Electrochemical Workstation. XPS was performed on Thermo Scientific K-Alpha spectrometer.

Reagents. Anhydrous CH_2Cl_2 was obtained using BRAUN MB-SPS solvent purification system. HPLC grade toluene and acetonitrile were purchased from Fisher and anhydrous propylene carbonate (PC) from Aldrich. Bu_4NPF_6 (electrochemical grade) was purchased from Fluka. Compounds **1a** and **1b** were synthesized according to previously reported procedure.[24]

Quantum Yield (Φ) of 2a and 3a. Fluorescence quantum yield of **2a** was measured in CH_2Cl_2 using 9,10-diphenyl anthracene in cyclohexane as a standard[25] and fluorescein in 0.1 M NaOH as a standard,[26] respectively.

Electrochemical Synthesis of Polymer Films. The polymers were electropolymerized from the 3.5 mM solutions of **1a** and **1b** in CH_2Cl_2 or toluene/acetonitrile (4:1) mixtures with Bu_4NPF_6. Ag/AgCl or Ag wire served as reference electrodes, Pt gauze as counter electrodes. Pt disk or indium tin oxide- (ITO-) coated glass were used as working electrodes. The electropolymerization was performed using cyclic voltammetry and sweeping voltage at scan rate of 30 mV/s. The working electrodes were then taken out and rinsed with CH_2Cl_2 or toluene and acetonitrile correspondingly. To eliminate the possible effect of fluoride in deborylation reaction, the electropolymerization was also performed using Bu_4NClO_4 supporting electrolyte, leading to identical polymers.

Spectroelectrochemistry. For spectroelectrochemical measurements, ITO derivatized with polymer **4a** was immersed in a 1 cm quartz cuvette containing 0.1 M Bu_4NPF_6/PC. Pt gauze and Ag wire were placed in the same cuvette as the counter and pseudoreference electrodes, respectively. The potentials were then set to the ITO electrode and the spectral absorption was recorded after the doping/dedoping was complete (evaluated by dropping of the current, ca. 2−3 min).

Electrochemical Characterization. Electrochemical investigations of compounds **1a**, **2a**, and **3a** were conducted in anhydrous CH_2Cl_2, with Bu_4NPF_6 (0.1 M) electrolyte, a Pt disk (d = 1.6 mm) as the working electrode, platinum wire as the auxiliary electrode and Ag/AgCl or Ag wire as the reference electrode. The electrochemical characterization of polymer films **4a** and **4b** on Pt disk electrodes were performed in anhydrous CH_2Cl_2, acetonitrile, and PC using platinum wire as the auxiliary electrode and Ag wire as pseudoreference electrode, with 0.1 M Bu_4NPF_6 as supporting electrolyte. The electrolyte solution was purged with Ar gas before and between electrochemical measurements. The Fc/Fc^+ redox couple was used as an internal standard.

Controlled Potential Electrolysis. Bulk electrolysis of **1a** and **1b** (10 mg in 6 mL) was performed using a home-built electrochemical cell with two compartments separated by porous frit. One compartment contained working Pt mesh (52 mesh, 3 × 1 cm^2) working electrode and Ag wire pseudoreference electrode, separated from the solution by a vycor tip. The other compartment contained counter Pt mesh electrode. The cell was purged with argon gas and kept under argon atmosphere for the entire experiment. Bulk electrolysis was performed at room temperature in anhydrous CH_2Cl_2 with Bu_4NPF_6 as supporting electrolyte, at 1.5 V versus a Ag wire pseudoreference electrode. After oxidative electrolysis, the solution was reduced at 0 V. Finally, electrolysis products **2a**, **3a**, and **2b** were purified by prep-Silica TLC using hexane/CH_2Cl_2 (2:1) mixture as an eluent.

2a. ^{1}H NMR (500 MHz, acetone-d_6, ppm): 9.23 (br s, NH_2), 7.91 (m, 2H, o-Ar−H), 7.76 (d, J = 5.1 Hz, 1H; th−H), 7.67 (d, J = 5.4 Hz, 1H; th−H), 7.52 (m, 2H, o-Ar−H), 7.51 (d, J = 5.1 Hz, 1H; th−H); 7.49−7.42 (m, 3H, m-, p-Ar−H), 7.35 (d, J = 5.4 Hz, 1H; th−H); 7.33 (m, 2H, m-Ar−H); 7.27 (m, 1H, p-Ar−H), 4.75 and 4.78 (NH). HRMS (ESI^-): calculated for $C_{24}H_{16}N_2BS_3$ (M − H), 439.05741; found, 439.05829.

3a. ^{1}H NMR (500 MHz, acetone-d_6, ppm): 9.20 (br s, NH_2), 7.85 (m, 4H, o-Ar−H), 7.71 (d, J = 5.0 Hz, 2H; th−H), 7.56 (s, 2H; th−H), 7.54 (m, 2H, o-Ar−H), 7.46 (d, J = 5.0 Hz, 2H; th−H); 7.43−7.37 (m, 3H, m-, p-Ar−H), 7.32 (m, 2H, m-Ar−H); 7.26 (m, 1H, p-Ar−H), 4.87 (br, NH); HRMS (ESI^+): calculated for $C_{48}H_{33}N_4B_2S_6$ (M + H), 879.12101; found, 879.12041.

RESULTS AND DISCUSSION

When exploring functionalization of azaborines **1**[24] we have observed their instability toward strong nucleophiles (BuLi), bases (LDA) and electrophiles (Br_2). Chemically irreversible multiredox electrochemical behavior with the first oxidation wave at E_{pa} = 0.48 V vs Fc/Fc^+ was also observed in cyclic voltammetry (CV) experiments.[27] However, while electrochemical oxidation in thiophene derivatives with free (unsubstituted) 2,5 positions, including terthiophene, usually leads to formation of conjugated polythiophene, we have not observed any polymer growth when potential was cycled at the first oxidative wave (up to 0.80 V vs Fc/Fc^+). Nevertheless, extending the potentiodynamic range to the second oxidation peak (above 1 V) led to growth of the polymer film on the anode (Figure 1).

The electropolymerization was found to occur in two solvent systems, toluene/acetonitrile (Figure 1a) and CH_2Cl_2 (Figure S3, Supporting Information) as evidenced by current increase with each cycles. The electrochemical behavior of the resulting polymer films in monomer-free solutions in CH_2Cl_2, as well as propylene carbonate (PC) and acetonitrile, exhibited chemically reversible p- and n-doping (Figures 1 and Figures S1, S2, and S4

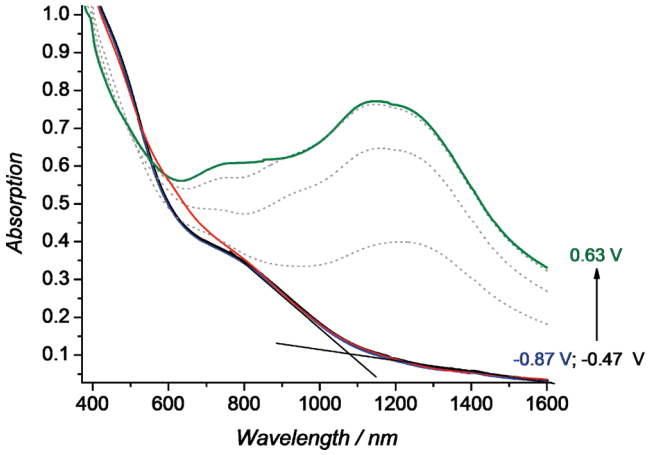

Figure 2. Spectroelectrochemistry (in PC/Bu_4NPF_6) of polymer film grown on ITO glass from **1a**. Vis−NIR spectra were taken at −0.87 V (black curve) and −0.47 V (blue curve); at −0.47 V after n-doping (red curve); at 0.18, 0.33, and 0.48 V (gray dotted curves); and at 0.63 V (green curve) vs Fc/Fc^+.

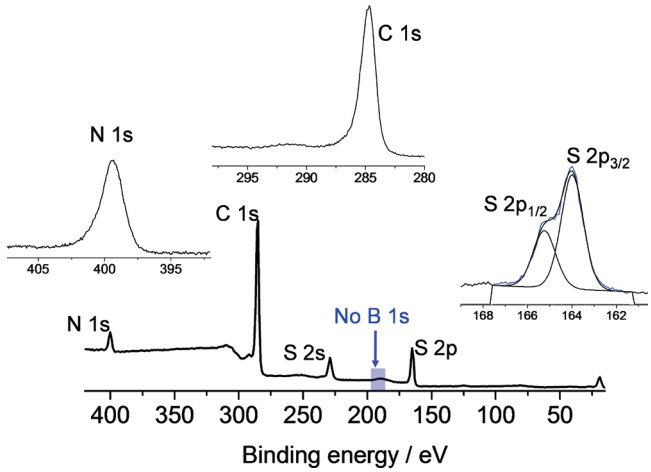

Figure 3. XPS of polymer film **4a** (undoped) grown on ITO from the solution of **1a**.

in the Supporting Information). The n-doping in CH_2Cl_2 and PC, however, becomes evident only after a few cycles, most likely due to the slow intercalation of the countercations in the initially dense film.[28] (Figure 1).

Differential pulse voltammetry (DPV) of the polymer films on Pt electrodes in monomer free solutions was used to determine electrochemical gaps of the polymer which was 1.17 and 1.24 eV for polymers grown from **1a** and **1b**, respectively (Figure S4, Supporting Information). The polymer was also grown potentiodynamically on ITO from the solution of **1a** in CH_2Cl_2 or toluene/CH_3CN resulting in dark brown shiny film. Its spectroelectrochemical characterization, performed in PC/Bu_4PF_6, showed strong absorption in 300−600 nm region and a distinct shoulder at ∼800 nm that extends into NIR region in the neutral, undoped state of the polymer (−0.47 V vs Fc/Fc^+, black solid line, Figure 2). Reducing the potential to −0.87 V vs Fc/Fc^+ had no effect on the absorption profile which confirmed the neutral state of the polymer. Upon electrochemical p-doping at increasing positive potentials, the absorption below ∼550 nm slightly bleached, while the polaron/bipolaron bands with maximum at 1145 nm and a shoulder at 770 nm grew significantly. This p-doping process is fully reversible and setting the potential back to −0.47 V vs Fc/Fc^+ recovers the original spectrum. The vis−NIR spectrum of polymer film was also taken after four cycles of electrochemical n-doping within −0.47 to −2.07 V vs Fc/Fc^+. The absorption of the neutral polymer after n-doping cycles, shown by the red curve in Figure 2, was almost identical to that in the neutral state after p-doping with slight increase in absorption at ∼600 nm which can likely be attributed to residual n-doping (or partial decomposition at highly negative potentials). This further proves that the 800 nm shoulder is the optical property of the neutral polymer, rather than the residual absorption of polarons formed during p-doping.

The optical bandgap estimated from the onset of this shoulder was 1.13 eV, which is in good agreement with the electrochemical gap. Such low band gap (E_g) was not expected for conjugated poly(**1**). In fact, DFT calculations (B3LYP/6-31G(d) level) of a series of oligomers $(\mathbf{1a})_n$, n = 1, 2, 3, 4, 6 predicts convergence of the E_g for the polymer at 2.1 eV (see the Supporting Information).

To elucidate the possible structure of the obtained polymer films an XPS analysis was conducted on dedoped samples (Figure 3). Surprisingly, the XPS clearly showed the absence of boron, while the C, S and N peaks, at the ratio equal to that in the monomer (24:3:2) and with expected energies, were observed. Together with electrochemical and optical properties of the polymer film, these data are consistent with formation of a conjugated polythiophene without boron substituents.

Interestingly, the thin-layer chromatography (TLC) analysis of the residual solution left from electropolymerization showed the presence of two new fluorescent species (Figure 2), while the color of the postpolymerization solution changed from yellow to brown. Suspecting that these new products might be intermediates to formation of the boron-free polymer, we have decided to elucidate the structures of the compounds formed during electrochemical reaction at the first oxidation wave.

Controlled potential electrolysis of solutions of thienoazaborines **1** was performed at potential 100 mV more positive than that of the first oxidation wave. After transferring the charge equivalent to ∼$2e^-$ per mole, the electrolysis was stopped and the solution was reduced back to 0 V. The TLC analysis of the resulting electrolysis mixture showed the depletion of the starting material and appearance of the two previously mentioned products that were isolated by preparative TLC in CH_2Cl_2/hexane mixture.

^1H NMR spectra of **1a** and two of its electrolysis products **2a** and **3a** in acetone-d_6 are shown in Figure 4. Symmetric structure with only one type of phenyl ring is apparent from the proton resonance of **1a**, with the Ph ortho protons positioned downfield (∼0.4 ppm) compared to meta and para protons, due to electron-withdrawing influence of the boron. The two types of thiophene protons are exhibited as doublets at 7.85 and 7.65 ppm. The NMR of the first electrolysis product, however, clearly shows desymmetrization through the presence of two different phenyl rings and four types of thiophene protons at 7.76, 7.67, 7.51, and 7.35 ppm. The observed chemical shifts and unchanged splitting of the thiophene protons is most consistent with a 1,2-σ shift of the Ph group displacing the electron-withdrawing boron substituent in one of the thiophene ring. The azaborine NH protons are slightly shifted upfield and a new type of NH signal appears at ∼4.8 ppm in the area of aromatic amines. The ^{11}B NMR signal at 34.1 ppm is identical to that for **1a** indicating the presence of the B═N moiety. On the basis of these observations

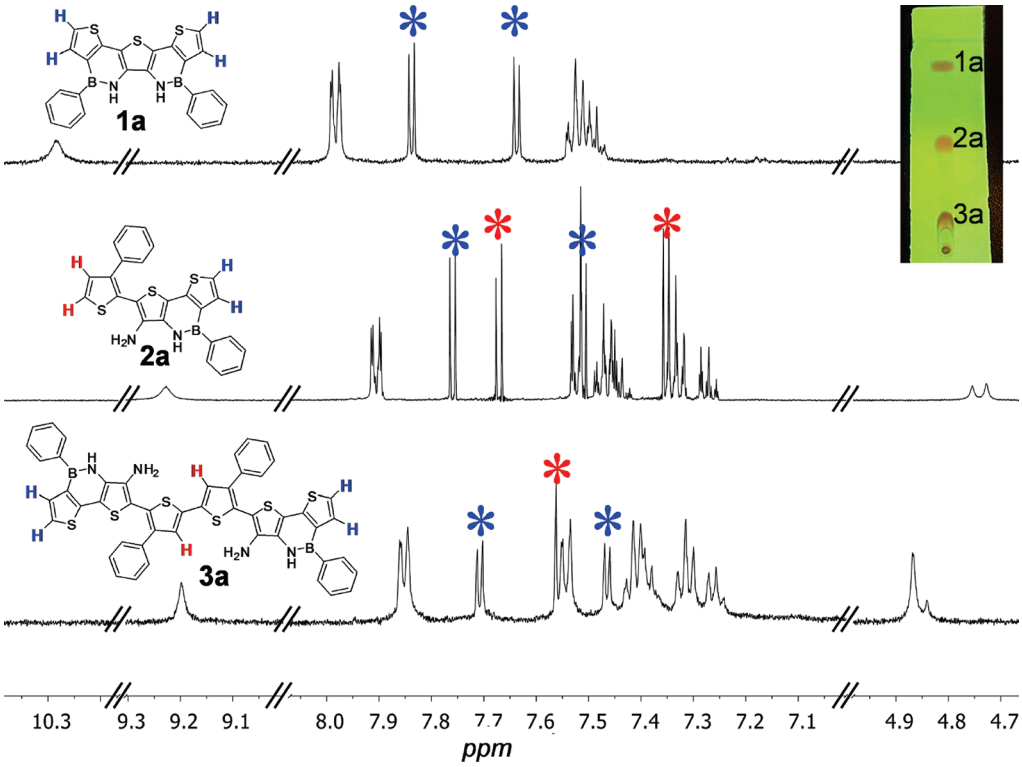

Figure 4. ^{1}H NMR spectra of **1a** and its electrolysis products **2a** and **3a** in acetone-d_6. TLC of the electrolysis mixture is shown in the inset.

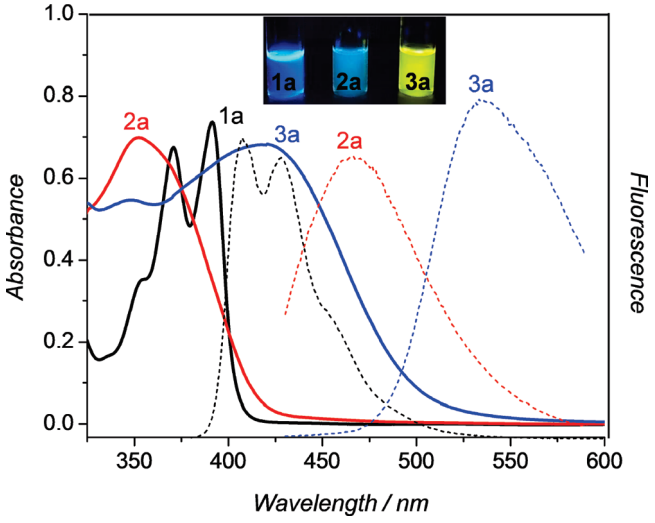

Figure 5. UV−vis absorption and fluorescence spectra of the compounds **1a**, **2a**, and **3a** in CH_2Cl_2.

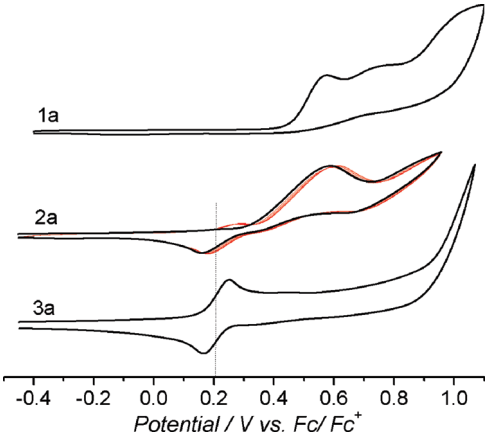

Figure 6. CVs of compounds **1a**, **2a**, and **3a** in CH_2Cl_2, 0.1 M Bu_4NPF_6. Red curves represent repetitive potential cycling of **2a** during which the appearance of **3a** is observed.

and accurate mass measurement in ESI−MS, we assigned structure **2a** to this product.

The ^{1}H NMR of the second electrolysis product still exhibited the presence of two different phenyl rings but pattern of thiophene protons have changed to two doublets (4H) and one new singlet at 7.57 ppm (2H). Such splitting together with high-resolution ESI−MS indicated dimerization of the intermediate **2a** into the sexithiophene derivative **3a**.

Therefore, the chemical reaction occurring during the first oxidation process must be accompanied by boron elimination and the formation of a new C−C bond between the thiophene and phenyl rings. Such irreversible redox behavior is not universal for azaborines. 3,6-Di(5-phenylpyrrol-2-yl)-1,2-dihydro-1,2-azaborine was earlier shown to form a stable radical cation in which the B−C bond remained intact, as evidenced by its reversible oxidative electrochemistry.[29] On the other hand, rearrangements with cleavage of the B−C bond, brought about by strong Lewis acidity of the boron center, have been described in the literature.[30] For example, Davies et al. has reported C−C coupling of thiophene fragments during chemical oxidation of nitrogen-coordinated dithienylboron derivatives.[31] More recently, Wang et al. described intramolecular rearrangement with

Scheme 1. Proposed Formation of the Electrochemical Products

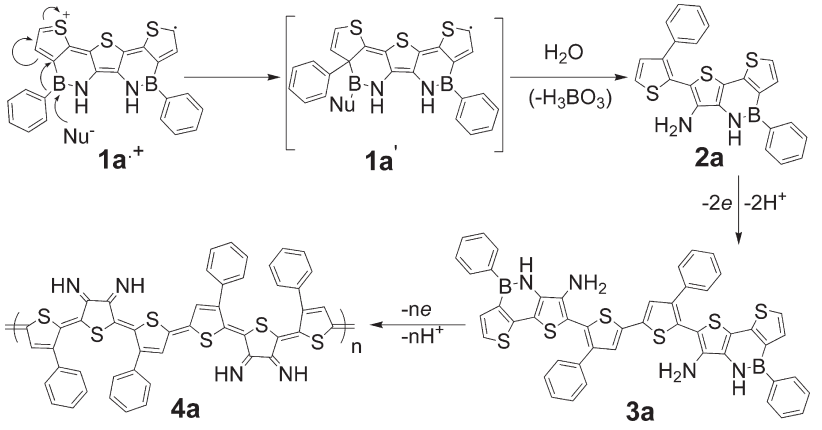

Ph-Ph bond formation and expulsion of the boron upon photooxidation of a structurally related nitrogen-stabilized boroaromatic derivative.[32,33] In our case, significant concentration of HOMO density on the boron atom, as predicted by DFT,[24] should drastically increase the reactivity of boron-containing moiety in the radical cation state ($\mathbf{1}^{\bullet+}$) and facilitate such transformations.

The electrochemical properties of **2a** and **3a** (Figure 6) are consistent with their structures and further support the proposed polymerization mechanism. Similar to **1a**, compound **2a** shows irreversible oxidation process at 0.57 V vs Fc/Fc^+, while compound **3a** exhibits a reversible oxidation at 0.21 V vs Fc/Fc^+. The appearance of a new peak at 0.21 V upon cathodic swipe of **2a** seem to indicate that the first oxidation process in **2a** does not lead to boron elimination, but rather radical coupling process to produce dimer **3a** (as in usual thiophene polymerization). The reversible redox behavior of **3a** can be explained by localization of the radical cation on the electron rich central diphenylbithiophene moiety. However, loss of the second electron at higher positive potential should lead to opening of the azaborine cycle and trigger further polymerization. In fact, polymer films analogous to those obtained from **1a** have been grown from **3a** (Figure S3, Supporting Information) when cycling is extended to higher potential (to 1.07 vs Fc/Fc^+).

The optical properties of electrolysis products **2a** and **3a** were probed by UV−vis and fluorescence spectroscopy in CH_2Cl_2 (Figure 5). The out-of-plane twist of the deborylated thiophene ring in **2a** caused by steric effect of the Ph substituent (see DFT calculations in the Supporting Information) leads to hypsochromically shifted absorption (λ_{max} = 352 nm, log ε = 4.1) and smeared fine vibronic structure as compared to the starting azaborine **1a** (391 nm). The dimerized **3a**, however, is red-shifted compared to both **1a** and **2a** with λ_{max} 420 nm (log ε = 4.0) due to extension of the conjugation. This trend in the absorption is reproduced by TD-DFT calculations that predict the HOMO−LUMO nature of the longest absorption of all three compounds, with λmax of 379, 373 nm, and 466 nm for **1a**, **2a**, and **3a**, respectively.

The fluorescence spectra of **2a** and **3a** exhibit large Stokes shifts of 0.9 and 0.6 eV correspondingly (**2a**, $\lambda^{em}{}_{max}$ 466 nm, photoluminescence quantum yield Φ_{PL} = 3.5%; **3a**, $\lambda^{em}{}_{max}$ 532 nm, Φ_{PL} = 6.5%) which points to large structural rearrangements in the excited state. This is very consistent with the expected charge transfer character and planarization of the excited states for such donor−acceptor molecules. The emission color shifts from the deep-blue for **1a** to sky-blue for the deborylated **2a** and bright-green-yellow for the dimer **3a**.

The FT-IR (see the Supporting Information) of the polymer **4a** shows vibrational N−H and aromatic C−H bands at 3350 and 3050 cm^{-1}, respectively, and a strong band at 1350 cm^{-1} due to C−C stretching in the polythiophene backbone. Also, the fingerprint region shows substantial similarity between the polymer **4a** (bands at 700, 750, and 850 cm^{-1}) and sexithiophene **3a**.

Put together, the above observations allow the proposal of the polymerization mechanism and the structure of the resulting polymer **4**, as depicted in the Scheme 1. The reaction is likely to start with nucleophilic attack of electrolyte anions on boron center in $\mathbf{1a}^{\bullet+}$, followed by thiophene-thiophene coupling similar to known aryl−aryl coupling of tetracoordinate boron compounds.[31,34] Subsequent reaction of unstable **1a**′ with nucleophiles and traces of water leads to boron expulsion and restores aromaticity of the reacting thiophene ring. Following electrochemical oxidation of the resulting **2a** causes its dimerization into **3a**. While one-electron oxidation of **3a** produces stable radical cation on the central bithiophene unit, the loss of the following electron(s) gives rise to deborylation of the terminal thiophenes, ultimately leading to polymer **4a**. Polymerization of **1b** appears to follow the same mechanism and the corresponding intermediate **2b** was isolated and characterized by NMR and ESI−MS spectroscopies (Supporting Information).

We note that amino-substituted ($-NH_2$) structure of **2a** and **3a** (as compared to imino-functionality $=$NH, as in **4a**) is not necessarily formed during electropolymerization, but possibly during isolation of the intermediates. On the other hand, the oxidized quinodiimine form of diaminothiophene moiety in **4a** is more consistent with the lack of spectroscopic or electrochemical response of **4a** to exposure of weak acids (dilute TFA) or reaction (overnight heating) with glyoxal.[35] Furthermore, the bandgap of the polymer **4a** (∼1.2 eV) is substantially lower than that of other polythiophenes bearing phenyl substituents (>2 eV)[36,37] and that of poly(diaminoterthiophene).[35] This band gap reduction, however, is expected for the structure of **4a** (see the Supporting Information) with alternating donor (diphenylbithiophene) and acceptor (thienoquinodiimine) moieties and combines the donor−acceptor and quinoidal approaches for the band gap reduction in conjugated polymers.[38−43]

dx.doi.org/10.1021/ma200503f |*Macromolecules* 2011, 44, 4729–4734

CONCLUSIONS

In summary, we have investigated the electrochemical behavior of fused thienodiazaborine systems. The electrochemical oxidation of these compounds leads to structural rearrangements, in particular, the transfer of the phenyl group onto thiophene ring and elimination of boron. This process is followed by oxidative coupling of the deborylated thiophene groups to form sexithiophene **3** and, eventually, a new boron-less polythiophene **4**. The donor−acceptor interactions and reduced aromaticity of the thienoquinodiimine moiety in polymer **4** significantly decreases its bandgap and leads to reversible p- and n-doping within the readily accessible potential window. Although the use of polymer **4** as a low band gap semiconductor will likely be limited by its nonplanar structure (caused by repulsion of Ph substituents), the approach should be applicable to other thienoazaborines with different substitution pattern and could eventually lead to new high-performance materials. On a more general note, this work sets an example of how isolating soluble intermediates of electrochemical polymerization can help elucidating the structure of insoluble polymers.

ASSOCIATED CONTENT

Supporting Information. Additional CV and DPV of polymer **4a** and **4b**; ESI−MS spectra of compounds **2a**, **3a** and **2b**; ^{1}H NMR of **2b**; FTIR of **1a**, **2a**, **3a**, and **4a**; DFT calculations of hypothetical $(\mathbf{1a})_n$ oligomers and HOMO−LUMO gap convergence correlation; calculated structures, HOMO/LUMO energies of intermediates **2a** and **3a**; DFT calculations of the oligomers $(\mathbf{4a})_n$ with the proposed polymer structure. This material is available free of charge via the Internet at http://pubs.acs.org/.

AUTHOR INFORMATION

Corresponding Author

*E-mail: (O.L.) olena.lukoyanova@mail.mcgill.ca; (D.F.P.) dmitrii.perepichka@mcgill.ca.

ACKNOWLEDGMENT

This work was supported by NSERC of Canada. The authors acknowledge Nadim Saade for mass spectrometry analyses.

REFERENCES

(1) Audebert, P.; Miomandre, F. In *Conjugated Polymers. Theory, Synthesis, Properties, and Characterization*, 3rd ed.; Skotheim, T. A., Reynolds, J. R., Eds.; CRC Press: Boca Raton, FL, 2007; p18−1.
(2) Roncali, J. *J. Mater. Chem.* **1999**, *9*, 1875–1893.
(3) Reddinger, J. L.; Reynolds, J. R. *Chem. Mater.* **1998**, *10*, 1236–1243.
(4) Steckler, T. T.; Abboud, K. A.; Craps, M.; Rinzler, A. G.; Reynolds, J. R. *Chem. Commun.* **2007**, 4904–4906.
(5) Tsuie, B.; Reddinger, J. L.; Sotzing, G. A.; Soloducho, J.; Katritzky, A. R.; Reynolds, J. R. *J. Mater. Chem.* **1999**, *9*, 2189–2200.
(6) Song, C.; Walker, D. B.; Swager, T. M. *Macromolecules* **2010**, *43*, 5233–5237.
(7) Patra, A.; Wijsboom, Y. H.; Leitus, G.; Bendikov, M. *Org. Lett.* **2009**, *11*, 1487–1490.
(8) Wijsboom, Y. H.; Sheynin, Y.; Patra, A.; Zamoshchik, N.; Vardimon, R.; Leitus, G.; Bendikov, M. *J. Mater. Chem.* **2011**, *21*, 1368–1372.
(9) Zhang, K.; Tieke, B.; Forgie, J. C.; Vilela, F.; Parkinson, J. A.; Skabara, P. J. *Polymer* **2010**, *51*, 6107–6114.
(10) Forgie, J. C.; Skabara, P. J.; Stibor, I.; Vilela, F.; Vobecka, Z. *Chem. Mater.* **2009**, *21*, 1784–1786.
(11) Forgie, J. C.; Kanibolotsky, A. L.; Skabara, P. J.; Coles, S. J.; Hursthouse, M. B.; Harrington, R. W.; Clegg, W. *Macromolecules* **2009**, *42*, 2570–2580.
(12) Wakamiya, A.; Mori, K.; Yamaguchi, S. *Angew. Chem., Int. Ed.* **2007**, *46*, 4273–4276.
(13) Yamaguchi, S.; Wakamiya, A. *Pure. Appl. Chem.* **2006**, *78*, 1413–1424.
(14) Jäkle, F. *Chem. Rev.* **2010**, *110*, 3985–4022.
(15) Hudnall, T. W.; Chiu, C. W.; Gabbai, F. P. *Acc. Chem. Res.* **2009**, *42*, 388–397.
(16) Zhou, G.; Baumgarten, M.; Mullen, K. *J. Am. Chem. Soc.* **2008**, *130*, 12477–12484.
(17) Wakamiya, A.; Taniguchi, T.; Yamaguchi, S. *Angew. Chem., Int. Ed.* **2006**, *45*, 3170–3173.
(18) Caruso, A.; Siegler, M. A.; Tovar, J. D. *Angew. Chem., Int. Ed.* **2010**, *49*, 4213–4217.
(19) Bosdet, M. J. D.; Jaska, C. A.; Piers, W. E.; Sorensen, T. S.; Parvez, M. *Org. Lett.* **2007**, *9*, 1395–1398.
(20) Bosdet, M. J. D.; Piers, W. E. *Can. J. Chem.* **2009**, *87*, 8–29.
(21) Nicolas, M.; Fabre, B.; Marchand, G.; Simonet, J. *Eur. J. Org. Chem.* **2000**, 1703–1710.
(22) Douglade, G.; Fabre, B. *Synth. Met.* **2002**, *129*, 309–314.
(23) Gronowitz, S.; Ingemar, A. *Chem. Scr.* **1983**, *22*, 55–59.
(24) Lepeltier, M.; Lukoyanova, O.; Jacobson, A.; Jeeva, S.; Perepichka, D. F. *Chem. Commun.* **2010**, *46*, 7007–7009.
(25) Hamai, S.; Hirayama, F. *J. Phys. Chem.* **1983**, *87*, 83–89.
(26) Lakowicz, J. R. *Principles of Fluorescence Spectroscopy*, 2nd ed.; Kluwer Academic/Plenum Publishers: New York, London, Moscow, and Dordrecht, The Netherlands, 1999.
(27) The first oxidation potentials of compounds **1a**,**b** in CH_2Cl_2 are 0.48 V in Bu_4ClO_4 and 0.57 V in Bu_4NPF_6 vs Fc/Fc^+.
(28) Jenkins, I. H.; Rees, N. G.; Pickup, P. G. *Chem. Mater.* **1997**, *9*, 1213–1216.
(29) Taniguchi, T.; Yamaguchi, S. *Organometallics* **2010**, *29*, 5732–5735.
(30) Pelter, A.; Pardasani, R. T.; Pardasani, P. *Tetrahedron* **2000**, *56*, 7339–7369.
(31) Davies, G. M.; Davies, P. S.; Paget, W. E.; Wardleworth, J. M. *Tetrahedron Lett.* **1976**, *10*, 795–798.
(32) Amarne, H.; Baik, C.; Murphy, S. K.; Wang, S. N. *Chem.—Eur. J.* **2010**, *16*, 4750–4761.
(33) Rao, Y. L.; Amarne, H.; Zhao, S. B.; McCormick, T. M.; Martic, S.; Sun, Y.; Wang, R. Y.; Wang, S. N. *J. Am. Chem. Soc.* **2008**, *130*, 12898–12900.
(34) Pelter, A.; Williamson, H.; Gareth, D. M. *Tetrahedron Lett.* **1984**, *4*, 453–456.
(35) Zotti, G.; Zecchin, S.; Schiavon, G.; Vercelli, B.; Berlin, A. *Electrochim. Acta* **2005**, *50*, 1469–1474.
(36) Naudin, E.; El Mehdi, N.; Soucy, C.; Breau, L.; Belanger, D. *Chem. Mater.* **2001**, *13*, 634–642.
(37) Yohannes, T.; Lattante, S.; Neugebauer, H.; Sariciftci, N. S.; Andersson, M. *Phys. Chem. Chem. Phys.* **2009**, *11*, 6283–6288.
(38) Wudl, F.; Kobayashi, M.; Heeger, A. J. *J. Org. Chem.* **1984**, *49*, 3382–3384.
(39) van Mullekom, H. A. M.; Vekemans, J. A. J. M.; Havinga, E. E.; Meijer, E. W. *Mat. Sci. Eng. R* **2001**, *32*, 1–40.
(40) Kertesz, M.; Choi, C. H.; Yang, S. J. *Chem. Rev.* **2005**, *105*, 3448–3481.
(41) Bredas, J. L.; Heeger, A. J.; Wudl, F. *J. Chem. Phys.* **1986**, *85*, 4673–4678.
(42) Kitamura, C.; Tanaka, S.; Yamashita, Y. *Chem. Mater.* **1996**, *8*, 570–578.
(43) Roncali, J. *Chem. Rev.* **1997**, *97*, 173–205.